IEEE Access
Multidisciplinary ⋮ Rapid Review ⋮ Open Access Journal

Received December 15, 2020, accepted January 14, 2021, date of publication February 9, 2021, date of current version February 25, 2021.

Digital Object Identifier 10.1109/ACCESS.2021.3058090

Partial Discharges in Electrical Machines for the More Electrical Aircraft. Part III: Preventing Partial Discharges

ALBERTO RUMI[1], (Student Member, IEEE), LUCA LUSUARDI[2], (Member, IEEE), ANDREA CAVALLINI[1], (Senior Member, IEEE), MARCO PASTURA[3], DAVIDE BARATER[3], (Member, IEEE), AND STEFANO NUZZO[3], (Member, IEEE)

[1]Department of Electrical, Electronic and Information Engineering "Guglielmo Marconi," University of Bologna, 40136 Bologna, Italy
[2]Thyssenkrupps Presta AG, 9492 Eschen, Liechtenstein
[3]Department of Engineering "Enzo Ferrari," University of Modena and Reggio Emilia, 41125 Modena, Italy

Corresponding author: Stefano Nuzzo (stefano.nuzzo@unimore.it)

This work was supported in part by the Clean Sky 2 Joint Undertaking through the European Union's Horizon 2020 Research and Innovation Program under Agreement 785513.

ABSTRACT In this paper, the results obtained from lab tests on twisted pairs subjected to different voltage waveforms and atmospheric conditions are used to propose how to modify the IEC Std. 60034-18-41. The goal is to make the standard suitable for the More Electrical Aircraft (MEA). The results show that it is initially necessary to screen out materials through simple tests. The enhancement factors for temperature can be modified to consider reduced pressures and temperatures using a simple model. The aging enhancement factor can be reduced considering the reduced sensitivity of the partial discharge inception voltage (PDIV) at low pressures on the enamel thickness. Eventually, reference will be made to the drive discussed in Part I of this series to draw conclusions about the likelihood of partial discharge inception in a random wound stator and how to reduce it by modifying either the inverter or the stator insulation. Reference to a random wound motor is made throughout the paper.

INDEX TERMS Partial discharges, More Electrical Aircraft, wide bandgap devices, SiC inverter, qualification, aging.

I. INTRODUCTION

Partial discharge (PD) can lead organic insulation to breakdown in brief times [1], [2]. Part I and II of this series of publications [3], [4] discuss electrical stresses and PD inception in inverter-fed actuators. Since wide bandgap inverters are a promising technology to achieve high power densities in the MEA [5]–[8], the impact of pressure and wide bandgap inverter waveforms are analyzed in [4]. In this Part, measures to avoid the inception of PD throughout the service life of the insulation system are discussed.

To ensure the reliability of organic insulation systems used in rotating machines (Type I), the IEC issued the Std. 60034-18-41 [9]. Standard [9] suggests qualification procedures to make sure that the winding insulation remains PD-free during the entire service life. However, it does not consider insulation systems installed on airliners, possibly supplied by wide bandgap inverters. The low atmospheric pressures combined with high electrical stresses favor the inception of PDs, as discussed in much more detail in [4]. PDs are more likely to occur in random wound machines due to the uneven distribution of the inter-turn voltage and are detrimental for polymeric insulation [10]–[12]. Failure times of minutes have been observed when using bipolar waveforms having a switching frequency of 100 kHz.

The aim of this paper is to review [9] with the aim of making it suitable for drives employed in the MEA. The paper is organized as follows. Section II presents the typical weak points in random wound motors. Section III recalls the procedure suggested by the IEC to prevent early failures. Section IV offers suggestions on how the insulation can be improved, while Section V reviews the procedure for qualification and verification of industrial drives [9] in the light of the MEA. Section VI discusses the application of these concepts to the drive discussed in [3].

II. WEAK POINTS IN THE INSULATION SYSTEM

The following are the issues that are most likely to affect the reliability of inverter-fed random wound motors:

The associate editor coordinating the review of this manuscript and approving it for publication was Jenny Mahoney.

1) Low turn/turn PDIV due to a poor performance of the resin at elevated temperatures.
2) Cracks in the insulation due to different thermal expansion coefficients of the wire enamel and the impregnating resin.
3) Ineffective impregnation of the end-winding (resin can drip off the end-winding when the stator is moved from the impregnation autoclave to the oven for curing).
4) Cavities between conductors due to incomplete filling of the slots by the impregnation resin.
5) Misplaced or missing insulation films in the phase insulation (allowing winding wires from different phases to come in contact).

Issues (1) and (2) are related to the choice of materials (design), (3) and (4) to processing. Problems of type (5) are due to manufacturing and need be screened out by quality control on the complete stators.

PD inception might occur in service even if the new insulation system is PD free. This can be due to, as an example, the insulation shrinking under thermal aging [13]. Thus, ensuring that the system is PD free after manufacturing is not enough: it must stay PD free over thousands of hours of service. This last need is critical, as it entails selecting materials stable over time under multiple stresses. This is the role of the qualification tests described in [9]. The same standard specifies how to carry out tests on new stators ensuring their quality and reliability.

In the following, focus will be given to the possible failure modes of the turn/turn insulation, thus at the inception of PDs between winding wires at a different potential. This situation can arise in the presence of defects of type (1), (3), (4) and (5).

III. QUALIFICATION: THE IEC 60034-18-41

After PD inception, the residual lifetime of the insulation is very short. Accordingly, [9] treats PD inception and failure as the same event. The design (and manufacturing) of the insulation should ensure that the electrical stress is low enough in all parts of the insulation throughout the service life to avoid PD inception. From the practical point of view, [9] requires that the PDIV of the insulation is above some critical voltage levels, which are larger than the voltage stresses in service.

The critical voltage levels depend on the insulation sub-systems (Phase/Phase, P/P, Phase/Ground, P/G, and Turn/Turn, T/T) sketched in Fig. 1. They depend on the peak voltage applied to the insulation system increased by suitable enhancement factors, EF. As an example, an EF is introduced to deal with the evidence that PDIV decreases with aging. Let the peak voltage applied to the machine be 1. If the PDIV is slightly above 1, PD will not be incepted. However, due to aging, the PDIV might decrease to a lower value $X < 1$. To compensate for this reduction, it is required that the PDIV is equal or larger than $1/X$. In this case $EF \geq 1/X$.

The empirical equation used to derive the critical voltage levels V_c is provided in [9].

$$V_c = V_{dc} \times OF \times WF \times EF_{PD} \times EF_T \times EF_{Aging} \quad (1)$$

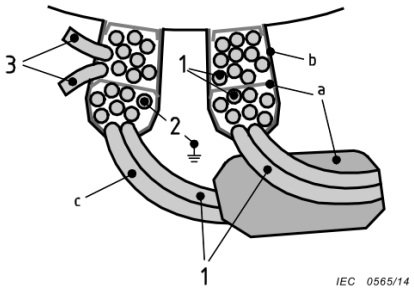

FIGURE 1. Rotating machine insulation subsystems: a P/P insulation, b P/G insulation, c T/T insulation (after [9]).

In (1)

- V_{dc} is the dc bus voltage of the inverter.
- OF is the Overshoot Factor, that is, the ratio of the peak voltage at the motor terminals to the dc bus voltage.
- WF is the Winding Factor which considers the distribution of the peak voltage in the P/P ($WF = 2$), P/G ($WF = 1.4$) and T/T ($WF = 0.7$) insulation. The WF reported here can be used when experimental results or simulations are missing.
- EF_{PD} is the PD safety factor accounting for the fact that PD extinction occurs at a voltage lower than PDIV (the PD Extinction Voltage). The standard suggests $EF_{PD} = 1.25$.
- EF_T is the temperature enhancement factor. It accounts for the fact that, as the temperature increases, the air density becomes lower favoring PD inception [14]. The suggested value is 1.3 for the T/T and P/P insulation. Due to the better cooling ensured by the contact with the stator, the P/G insulation temperature is lower. Thus, EF_T is set to 1.1 for the P/G insulation.
- EF_{Aging} models the progressive degradation of the insulation. Its value is calculated as $EF_{Aging} = \max(1, 1.2 \times T_s/T_c)$ where T_s and T_c are the service and class temperature, respectively.

For a drive having a given DC bus voltage, the OF will depend on the cable length, inverter rise time and cable/winding reflection coefficient [3]. Applying eqn. (1) to the various sub-systems leads to three critical voltage levels. Each sub-system should prove to be PD-free below the corresponding V_c. The EFs used in (1) are different for verification and qualification tests.

A. VERIFICATION TESTS

Verification tests are performed on new stators. When feasible, the P/P, P/G, and T/T should be tested as independently as possible. Tests of the P/G and P/P (if the star point is accessible) can be performed using AC sinusoidal voltages [9] following the schemes suggested in [15]. The T/T insulation can be tested using surge voltages with appropriate rise time, possibly comparable to that of the inverter used in operation [9]. A comprehensive summary of the testing options using surge voltages is reported in [16].

The quality of an insulation sub-system is verified if the system is PD-free below the corresponding V_c. This step

ensures that the design and the manufacturing procedure are good enough to prevent PD inception. The EF_{Aging} used in (1) should be larger than 1 to account for the fact that the insulation is new, and PDIV will decrease over time due to (mostly) thermal stress.

B. QUALIFICATION TESTS

Qualification tests are carried out to make sure that the decrease of PDIV with aging is not too fast. Qualification tests comprise sub-cycles where aging factors (thermal, mechanical, ambient) are applied sequentially (or simultaneously, if workable [17]). The IEC 60034-18-21 [18] is the reference to design the aging tests. At the end of each sub-cycle, a PD-proof test is carried out. In case PDs are incepted below V_c or the system breaks down (due e.g. to mechanically induced cracks [19]), the failure time is noted. Otherwise, another sub-cycle is performed. With this failure criterion, the IEC assumes that the residual time from PD inception to breakdown is negligible.

Qualification tests must be carried out on not less than five samples. To save money, it is customary to use insulation models (twisted pairs, motorettes) instead of complete stators. For qualification tests $EF_{Aging} = 1$ as the insulation is subjected to progressive aging, and it is not necessary to simulate its effects.

C. METHODS FOR PD TESTING

The results reported in Parts I and II of this series prove that the voltage waveform influences the voltage distribution within a system, but not the physics of the discharge, leading to the same PDIV. Thus, they confirm that both impulsive and AC voltage waveforms can be used if the peak-to-peak voltage distribution is the same in operation and during the tests [9].

For complete stators, AC voltages can be used for testing the P/G and P/P insulation. The insulation will be tested with all points at the same voltage level, regardless of the voltage distribution during operation. AC testing is thus a more conservative option than using surge generators.

The electrical stress applied to the T/T insulation is significant under inverter voltage waveforms and negligible under AC voltages. Thus, for testing the T/T insulation on complete stators, one must use surge generators. Surge generators provide a quantity, the Repetitive Partial Discharge Inception Voltage (RPDIV), which is defined as the minimum peak-to-peak impulse voltage at which more than five PD pulses occur on ten voltage impulses of the same polarity. The RPDIV exceeds the actual PDIV [20] as:

1. Surge generators create a large interference that tends to mask the PD pulses, reducing the detection sensitivity [21].
2. For most surge generators, the voltage impulses are unipolar with low repetition rate. This leads to a low PD inception probability. As a result, the voltage must be in excess of the PDIV to attain the RPDIV [20]. Figure 2 shows a comparison between the inception and extinction voltages measured on twisted pair (couples of winding wires twisted together) and subjected to different voltage waveforms. As can be seen, the RPDIV measured using a surge generator is higher and more sparce than the measurements obtained using different voltage sources.

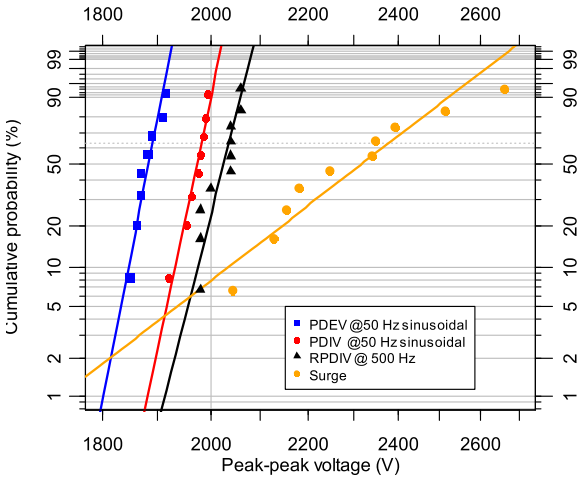

FIGURE 2. Example of PDIV, PDEV (Partial Discharge Extinction Voltage) and RPDIV values measured on twisted pairs using different high voltage sources. ▲ is obtained using a unipolar square voltage waveform having a repletion frequency of 500 Hz. The repetition rate of the surge voltage is 1 Hz.

According to [9], PDIV tests on insulation models can be carried out using sinusoidal voltages. This choice simplifies the testing procedure and ensures the best detection sensitivity. The possibility of using sinusoidal waveforms derives from the fact that, owing to the structure of the twisted pair, the potential difference between any couple of points (of the twisted pair) is the same using impulse or AC voltages, thus leading to the same PDIV.

IV. IMPROVING STATOR INSULATION

A. MATERIAL SELECTION BASED ON PDIV BEHAVIOR

Some impregnating resins affect the PDIV at operating temperatures. In the worst case, the PDIV of the impregnated wires can be lower than that of the bare wires at elevated temperatures. To screen out resins having poor performance at high temperatures, simple tests on insulation models consisting of winding wires twisted together (twisted pairs) according to [22] can be performed. The comparison of PDIV of impregnated and non-impregnated twisted pairs at room temperature and at elevated temperatures can help to discriminate which resins do not perform well.

As an example, comparative tests were carried out using AC 50 Hz sinusoidal waveforms with a 1 nF coupling capacitor [23]. A high frequency current transformer is coupled the PD pulses to a Techimp PDBase II detector. The voltage was raised in steps of 25 V each lasting 30 seconds. Tests were performed at room temperature and 140 °C. Since the PDIV corresponds to the minimum voltage to break the air gap in a twisted pair, the results of the test are displayed in a Weibull probability chart in Fig. 3. Figure 4 shows a

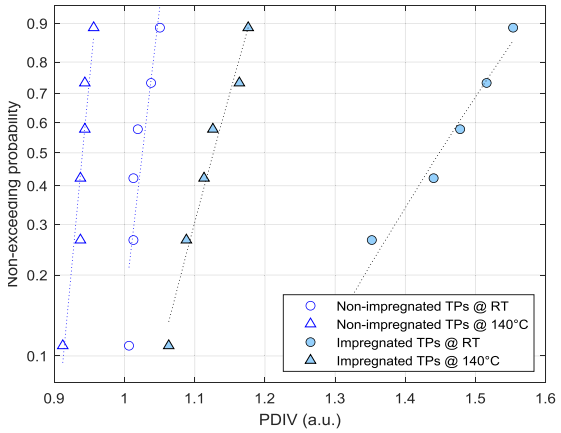

FIGURE 3. Weibull chart showing the experimental PDIV data at room temperature (RT) and 140 °C for both impregnated and non-impregnated twisted pairs. The data have been anonymized and are reported in per unit of a base value.

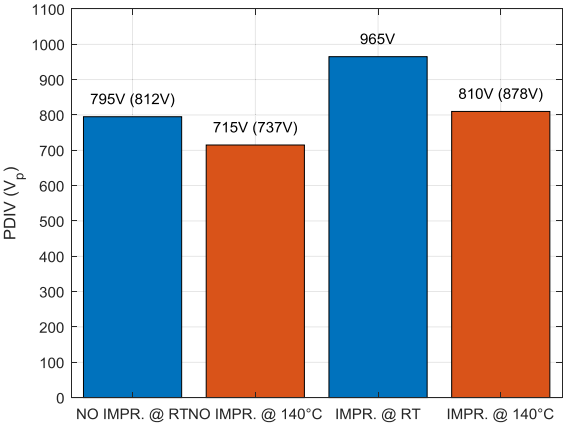

FIGURE 4. Comparison of PDIV at room temperature and 140 °C for non-impregnated and impregnated twisted pairs based on the 10% percentile of the Weibull curve fitting the experimental data. The numbers between parentheses are the predictions based on the model presented in [4].

summary of the PDIV data using the 10th percentiles of the Weibull distributions fitting the experimental data (B10). For the non-impregnated twisted pairs, the B10 PDIV at 140 °C is lower by ∼10%. The model presented in Part II of this series and reported here in (2) calculates the dependence of the PDIV on the air number density, $n_{P,T}$ (in m^{-3}) at pressure P and temperature T [4].

$$\frac{PDIV_{P,T}}{PDIV_{ref}} = 1 + 0.299 \ln \frac{n_{P,T}}{n_{ref}} + 0.0446 \left(\ln \frac{n_{P,T}}{n_{ref}} \right)^2 \quad (2)$$

In (2), n_{ref} is the number density corresponding to the pressure and temperature at the time the reference PDIV ($PDIV_{ref}$) was measured. The model predicts that the voltage should drop by ∼9% when the temperature is increased from RT to 140 °C. So, the lower PDIV at 140 °C of the non-impregnated twisted pairs (∼10%) can be explained by the lower air density.

For the impregnated twisted pairs, the reduction is ∼19%. The drop is larger, but still the PDIV exceeds that of the non-impregnated twisted pairs. This behavior is common.

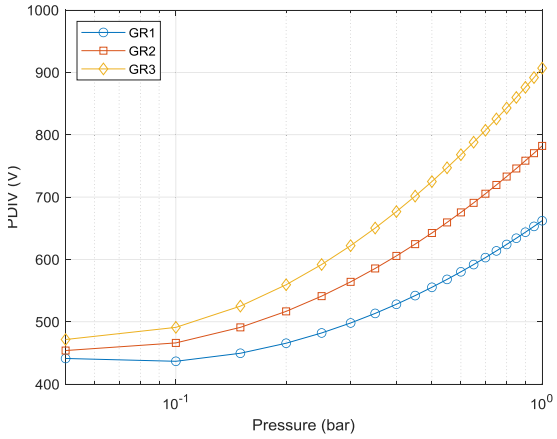

FIGURE 5. Difference between PDIV at room temperature (RT) for a GR2 and a GR3 winding wires ($\varnothing = 0.56$ mm, $\varepsilon_r = 2.7$) as a function of atmospheric pressure.

However, at elevated temperatures, cases have been reported where the impregnated twisted pairs display statistically lower PDIV values compared to non-impregnated twisted pairs. These resins should not be considered for MEA applications.

B. ENHANCE THE IMPREGNATION

The resin requirements to avoid problems of type (3) and (4) are at odds. On the one hand, the viscosity of the resin should be low to fill the slots completely, avoiding the formation of cavities. On the other hand, large resin viscosities help to avoid the flow of the resin in the end-winding when the stator is extracted from the autoclave and placed in the oven for curing.

A possible solution is to use a low-viscosity epoxy resin suitable for double impregnation. Alternatively, it is possible to encapsulate the end-winding. This solution however increases the weight of the actuator.

C. USING GRADE 3 WINDING WIRES WILL HELP?

Three different winding wire grades (grades 1-3) are available on the market [22]. Grade 3 wires are suitable for inverter duty. Provided that the slot fill factor does not become too low, it is reasonable to consider using Grade 3 wires. To compare the results achieved by wires having the same diameter (0.56 mm) but different grades, a software that couples FEM analysis of the electrostatic field with the streamer inception criterion calculated using MATLAB was used The factor K adopted in the streamer inception criterion is equal to 6, and was estimated from measurements performed in the lab on twisted pairs having different diameters and insulation thicknesses. The software is discussed in detail in [14] and summarized in the Part II of this series, thus it will not be described here. Figure 5 shows the results. At 150 mbar, the PDIV increases from 438 V (GR2) to 476 V (GR3), that is 38 V. The increase is limited (8.7%) and might not be a turning point to improve the design.

To further emphasize this result, Fig. 6 reports the PDIV values using those obtained by GR2 as the baseline, at

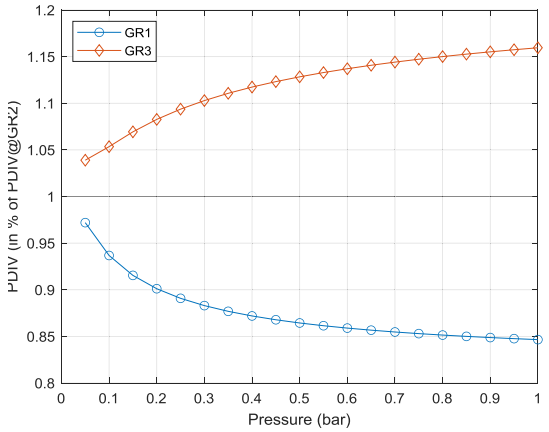

FIGURE 6. PDIV at room temperature for a GR1 and a GR3 winding wires ($\varnitothing = 0.56$ mm, $\varepsilon_r = 2.7$) as a function of atmospheric pressure. The PDIV are reported using the PDIV of a GR2 wire as a reference. The thickness of the insulation is 12.5μm, 23.5μm, and 35.5μm for the wires of grade 1, 2, and 3, respectively.

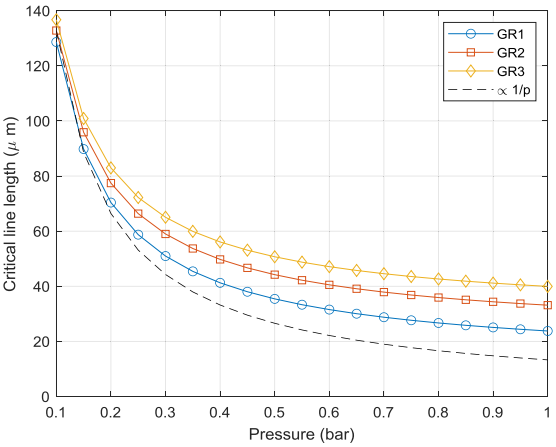

FIGURE 7. Critical line lengths for winding wires having different grades as a function of atmospheric pressure. The characteristics of the winding wires are the same reported in Fig. 6.

all pressures. As the pressure decreases, the dependence of PDIV on the enamel thickness becomes less significant. The improvement, equal to ∼16% at 1000 mbar, lowers to 8.7% at 150 mbar.

This behavior can be explained inspecting the electrical field lines where PD takes place (here indicated as critical field lines, CFL). The lengths of the CFLs as a function of the pressure are reported in Fig. 7. The CFLs follow approximately the reciprocal of the pressure. From the electrostatic partition of the voltage between the air and the solid insulation the voltage drop in the solid can be evaluated as:

$$E_{gas} \times l_{gas} + E_{solid} \times l_{solid} = V \rightarrow V_{solid} = E_{solid} \times l_{solid} \approx V\left(1 - \frac{l_{gas}}{l_{gas} + \varepsilon_r^{-1} l_{solid}}\right) \quad (3)$$

where E_{gas} and E_{solid} are the electric fields in the gas and in the solid, l_{gas} and l_{solid} are the lengths of the CFLs in the gas and in the solid. To derive (3), it is assumed that (a) the relative permittivity of the air is equal to 1, neglecting the changes due

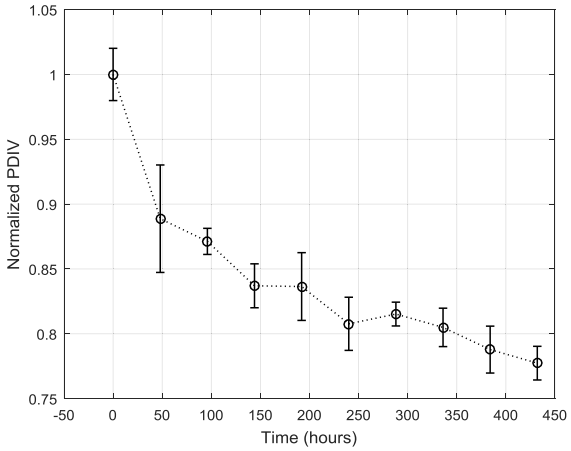

FIGURE 8. PDIV of twisted pairs during thermal aging at 230 °C. The plot shows the average values along with 95% confidence intervals.

to moisture content and temperature [24], and (b) the electric fields are constant and normal to the dielectric surfaces, thus $E_{gas} = \varepsilon_r \times E_{solid}$ where ε_r is the relative permittivity of the solid. The CFL length in the gas is $l_{gas} \approx$ k/p (see Fig. 7). The same will not happen for l_{solid}. Therefore, the lower the pressure, the longer l_{gas} and the lower the voltage drop in the solid insulation. Consequently, the role of the solid dielectric becomes less important at reduced pressures.

At low pressures, the reduced sensitivity of PDIV to the enamel thickness makes less attractive using Grade 3 magnet wires. However, at the same time, it de-emphasizes the impact of aging on the reduction of PDIV over time.

As mentioned in Section III, [9] considers a factor equal to $EF_{Aging} = \max(1, 1.2 \cdot T_s/T_c)$ to model the effects of thermal aging. This agrees with the results of thermal aging tests on class 200 winding wires aged at 230 °C [13]. Figures 8 and 9 show a simultaneous reduction of PDIV and of insulation thickness. The latter can be explained considering that volatile byproducts are expelled from the enamel at elevated temperatures reducing the insulation thickness [13]. The reduced sensitivity of PDIV on the solid insulation thickness at reduced pressure makes the impact of aging in MEA actuators less important than what experienced by industrial machines. Consequently, the enhancement factor for aging in (1) can be reduced. The logic to evaluate its value is presented in the next section.

V. MODIFY THE IEC 60034-18-41 TO FIT AIRCRAFT SPECIFIC CONDITIONS

Compared to industrial drives, actuators for the MEA have much different operating conditions. Figure 10 shows the joint probability density (JPDF) of the atmospheric conditions encountered by a commercial plane. The JPDF was estimated using all available data for the year 2015 in the IAGOS database [25]. Commercial aircraft spend most of the time at altitudes where the pressure is about 20 kPa (200 mbar) and temperatures from −60 °C and −40 °C.

Let the Reference Operating Condition (ROC) be the most challenging (for the insulation) combination of temperature

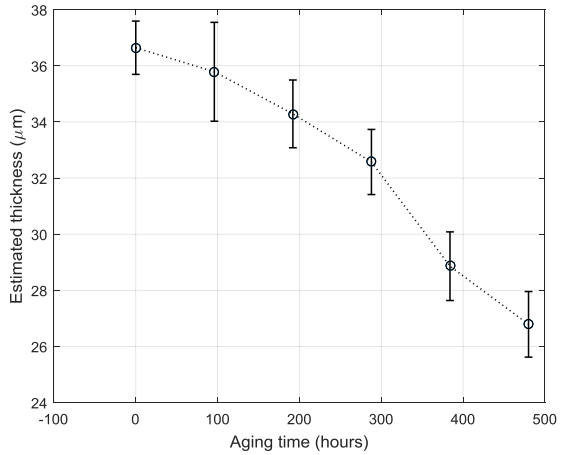

FIGURE 9. Enamel thickness of twisted pairs during thermal aging at 230 °C. The plot shows the average values along with 95% confidence intervals.

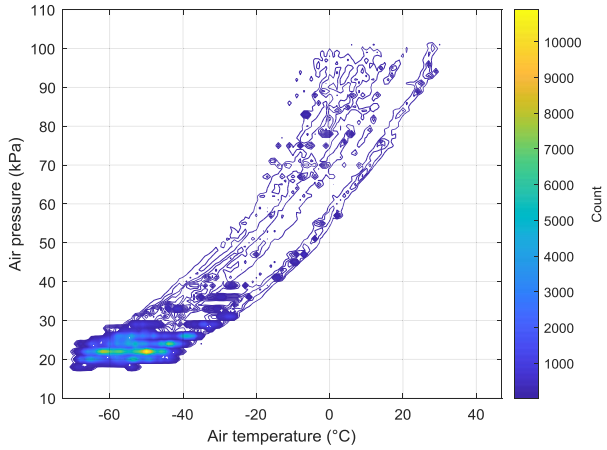

FIGURE 10. Joint probability density of air pressure and temperature [25].

and pressure experienced during the flight. Referring to Fig. 10, a reference value of 150 mbar can be assumed as a conservative figure for the pressure. As the reference temperature, one should consider the hot spot temperature of the motor. Here, it will be assumed that the hot spot temperature is 140 °C. Different mission profiles and machine designs can lead to different ROCs.

The ratio of the number density of the air at ROC to that at STP is:

$$\frac{n_{P,T}}{n_{STP}} = \frac{150\ \text{mbar}}{273+150\ \text{K}}\frac{273+25\ \text{K}}{1013\ \text{mbar}} = 0.108 \tag{4}$$

Using model (2), the PDIV at the ROC is 56% lower than the PDIV recorded at ground level:

$$\frac{PDIV\left(n_{P,T}\right)}{PDIV\left(n_{STP}\right)} = 0.56 \tag{5}$$

Assuming that the permittivity of the dielectric under aging and at elevated temperatures does not increase above 4, then EF_T in (1) can be replaced with an enhancement factor that depends on both temperature and pressure that, considering

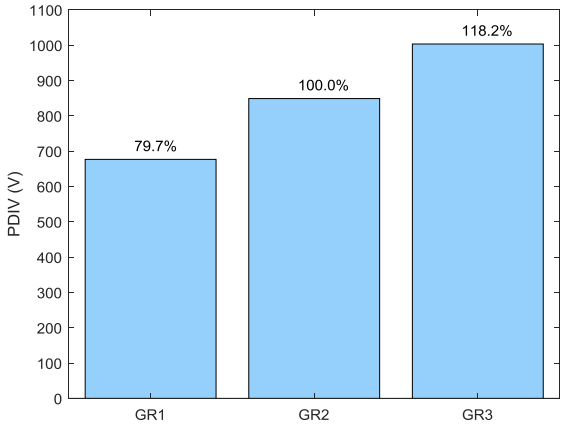

FIGURE 11. PDIV at room temperature and 1000 mbar for a GR1, GR2, and GR3 winding wires ($\emptyset = 0.56$mm, $\varepsilon_r = 2.7$).

the ROC, is:

$$EF_{P,T} = \frac{PDIV\left(n_{P,T}\right)}{PDIV\left(n_{STP}\right)} = 1.0/0.56 \approx 1.8 \tag{6}$$

Considering the large value of $EF_{P,T}$, if an insulation system is PD free at 150 mbar, it will also be PD free at the ground level. Therefore, design should be carried out using the ROC as primary input.

In order to fit [9] the peculiar conditions of actuators used in the MEA, the enhancement factor for aging should also be improved, taking into account the fact that the role of the enamel insulation in preventing PD activity becomes less important at high altitudes.

The standard suggests that, for an insulation system operating always at its class temperature, $EF_{Aging} = 1.2$. This figure implies a reduction of the PDIV over time of $1/1.2 = 83\%$. This is better than the reduction of PDIV achieved shrinking the insulation by 20μm, i.e. by selecting a grade 1 instead of a grade 2 winding wire, as shown in Fig. 11. Thus, to model the effect of thermal aging on PDIV it is possible to consider it akin to a reduction of the enamel thickness. Figure 6 shows that shrinking the enamel thickness from GR2 to GR1 causes a 9% reduction of PDIV at a pressure of 150 mbar. Therefore, the aging enhancement factor can be assumed to be:

$$EF_{Aging} = \max\left(1,\ 1.1 \times T_s/T_c\right) \tag{7}$$

VI. VI WORKING CASE

A. COMPARISON OF STRESS LEVELS WITH PDIV

The analysis considers the reference system described in [3], i.e., a low voltage random-wound motor used for the MEA. Using simulation tools that were fine-tuned based on experimental measurements on stators, the maximum turn-to-turn and turn-to-ground voltages were determined for different rise times and cable lengths in a range typical of MEA drives. The simulations consider the worst-case scenario, when the first turn is placed close to the last one within the stator slot. For the turn/turn insulation, the highest peak voltage (1.47 in per unit of the DC bus voltage) is found for a cable of 2 m length and a rise time lower than 25 ns, see Fig. 12. For the

TABLE 1. Estimation of limit DC bus voltage for the system described in [1]. Cable length = 2 m. Rise time = 23 ns.

Drive type	Levels	Insulation	U_{dc} (V)	OF	EF_{PD}	$EF_{p,T}$	EF_{Aging}	Total	PDIV (V)	$V_{dc,lim}$ (V)
0-Vdc	2	T/T	540	1.47	1.25	1.8	1.1	3.64	810	223
	2	P/G		1.51				3.74	1160	310
+-Vdc/2	2	T/T		1.47				3.64	810	223
	2	P/G		1.01				2.50	1160	464
+-Vdc/2	3	T/T		0.735				1.82	810	445
	3	P/G		0.755				1.87	1160	621
+-Vdc/2	5	T/T		0.367				0.91	810	890
	5	P/G		0.377				0.93	1160	1247

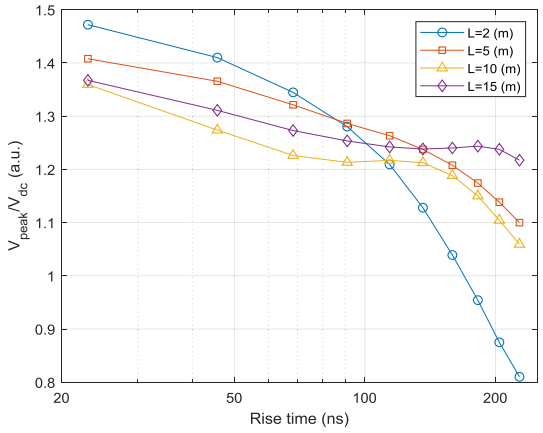

FIGURE 12. Turn/turn worst case voltage as a function of rise time and for different cable lengths.

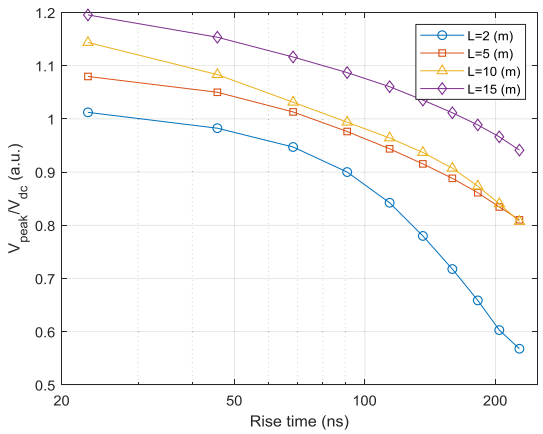

FIGURE 13. Phase/ground voltage as a function of rise time and for different cable lengths.

phase-to-ground insulation, the maximum overvoltage (1.2 in per unit of the dc bus voltage) occurs for a 15 meters-long cable with the rise time below 25 ns, see Fig. 13. As can be observed, both peak voltages are below the theoretical maximum (equal to two). This is because, for the considered drive system, the impedance mismatch between the cable and the machine limits the reflection coefficient to 1.85 depending on the frequency. For longer cables, the filtering contribution of the cable series inductance reduces the peak voltage.

In the following, the limit DC bus voltage ($V_{dc,lim}$) allowed for different inverter configurations will be evaluated. Following (1), $V_{dc,lim}$ will be defined as the DC bus voltage satisfying the equality V_c = PDIV for the insulation subsystem considered. Thus, each DC bus voltage equal or above $V_{dc,lim}$ will lead to the inception of PDs.

As drive type in Tables 1-4, a conventional two-level inverter with ground connection to the negative DC rail or to DC-link mid-point is considered. In the second case the converter's output voltage varies between ±Vdc/2. Three- and five-level inverters with the same ground configuration are also considered. The reference PDIV levels were derived based on measurements performed on twisted pairs (810 V_{peak}) or motorettes (1160 V_{peak}) dealing with the T/T or the P/G insulation, respectively. The overshoot factor,OF in Table 1 is derived from the model described in Part I of this series of publications. In (8), TE is the total enhancement of the DC voltage to derive the critical voltage level:

$$TE = WF \times OF \times EF_{PD} \times EF_{P,T} \times EF_{Aging} \tag{8}$$

Thus:

$$V_{dc,\mathrm{lim}} = PDIV/TE \tag{9}$$

One of the assumptions made to derive the analysis reported in the following is that the PDIV increment conferred by the impregnation process should not be considered in the design phase.

The reason behind this choice is that measurements performed on twisted pairs show that the PDIV of impregnated samples presents a large dispersion. An example of this behavior is reported in Fig. 3. Despite the randomness (due to the fact that the thickness of the impregnation changes from sample to sample), one could argue that PDIV has improved by 30% after impregnation.

However, given the complexity of a stator, the same does not happen always, and weak points might exist in the end-winding or at the slot entrance if the impregnating resin drips off during the transfer of the stator from the impregnation tank to the oven for curing.

Depending on the reliability of this process, one could relax this constraint. However, referring to Fig. 3, one should also consider that the increment of PDIV due to the resin at

TABLE 2. Estimation of limit DC bus voltage for the system described in [1]. Cable length = 15 m. Rise time = 23 ns.

Drive type	Levels	Insulation	U_{dc} (V)	OF	EF_{PD}	$EF_{p,T}$	EF_{Aging}	Total	PDIV (V)	$V_{dc,lim}$ (V)
0-Vdc	2	T/T	540	1.37	1.25	1.8	1.1	3.39	810	239
	2	P/G		1.7				4.21	1160	276
+-Vdc/2	2	T/T		1.37				3.39	810	239
	2	P/G		1.2				2.97	1160	391
+-Vdc/2	3	T/T		0.685				1.70	810	478
	3	P/G		0.85				2.10	1160	551
+-Vdc/2	5	T/T		0.342				0.85	810	953
	5	P/G		0.425				1.05	1160	1105

TABLE 3. Estimation of limit DC bus voltage for the system described in [1]. Cable length = 2 m. Rise time = 90 ns.

Drive type	Levels	Insulation	U_{dc} (V)	OF	EF_{PD}	$EF_{p,T}$	EF_{Aging}	Total	PDIV (V)	$V_{dc,lim}$ (V)
0-Vdc	2	T/T	540	1.12	1.25	1.8	1.1	2.77	810	292
	2	P/G		1.28				3.17	1160	366
+-Vdc/2	2	T/T		1.12				2.77	810	292
	2	P/G		0.78				1.93	1160	601
+-Vdc/2	3	T/T		0.56				1.39	810	584
	3	P/G		0.64				1.58	1160	732
+-Vdc/2	5	T/T		0.28				0.69	810	1174
	5	P/G		0.32				0.79	1160	1468

TABLE 4. Estimation of limit DC bus voltage for the system described in [1]. Cable length = 15 m. Rise time = 90 ns.

Drive type	Levels	Insulation	U_{dc} (V)	OF	EF_{PD}	$EF_{p,T}$	EF_{Aging}	Total	PDIV (V)	$V_{dc,lim}$ (V)
0-Vdc	2	T/T	540	1.24	1.25	1.8	1.1	3.07	810	264
	2	P/G		1.53				3.79	1160	306
+-Vdc/2	2	T/T		1.24				3.07	810	264
	2	P/G		1.03				2.55	1160	455
+-Vdc/2	3	T/T		0.62				1.53	810	528
	3	P/G		0.765				1.89	1160	613
+-Vdc/2	5	T/T		0.31				0.77	810	1056
	5	P/G		0.382				0.95	1160	1225

high temperature is much lower than what observed at room temperature.

For the measurements at 140 °C reported in Fig. 3, the increment offered by the resin is 810/715 = 1.13, that is in the range 10%-15%.

The results of these calculations are reported in Tables 1-4. The results underline that MEA applications having a DC bus voltage equal to 540 V can operate reliably when using three- or five-level inverter with split DC bus (±Vdc/2 configuration). However, with a three-level configuration, the turn-to-turn insulation can be overstressed ($V_{dc,lim}$ lower than U_{dc}) if the first and last turns of the first coil are close each other or in contact. This is the worst-case scenario considered in the results reported in Table 1-4. Due to the way that conductors are positioned in the slot during manufacturing of random windings, it is not possible to ensure that the first and the last turn are not in contact. Thus, the worst case should be the design target to ensure reliability and, therefore, only a five-level inverter can guarantee a reliable operation in all cases for the reference system analyzed. If higher DC bus voltage levels are sought, more complex solutions need be investigated.

B. POSSIBLE SOLUTIONS

The considerations reported above lead to the conclusion that the MEA and industrial drives should be designed differently. The target for MEA drives would be (a) maximizing the PDIV at the ROC while (b) reducing the electrical stress

applied to the turn/turn insulation. For point (a), one should bear in mind that increasing the insulation thickness might not provide significant improvements. Besides, point (a) can conflict with the maximization of the specific power (per unit volume or per unit weight). Regarding point (b), the inverter design could be tailored for this application although this might lead to more complex topologies, not only multi-levels which at the moment are not widely adopted for low voltage applications.

To deal with the voltage overshoot challenges and dv/dt stress, different design solutions can be identified at different drive levels.

Possible solutions may involve:

- Use of passive filters at the inverter output. This approach represents the most common solution adopted nowadays. With the insertion of RLC filters, a damping action is forced on the voltage overshoot ensuring a smooth variation. The drawbacks of this solution are multiple: an increased complexity of the system, increased volume of the inverter, increased component count and thus reduced reliability, and increased power losses [26].
- Innovative design of the inverter. This solution, often referred as active dv/dt filtering, may involve the use of active gate drivers, which basically slow down the commutation speed to maintain the voltage overshoot below a given threshold [27], [28]. This comes at the cost of increased switching losses and a reduced efficiency of the converter but has the advantage to tailor the converter dv/dt to the specific application layout. In alternative, innovative inverter architectures have been proposed to minimize the voltage overshoot at the motor terminal maintaining the advantage of fast devices' commutations [29], [30]. This is in general counterbalanced by an increase complexity, and an increment of the number of components. Conventional multilevel inverters are able to reduce overvoltages at the machine terminals, but the higher number of devices in series decreases the inverter reliability, shifting the bottleneck point from the winding insulation to the power electronics.
- Innovative design of the stator windings, considering new materials and windings structures for low voltage windings [31], [32]. One possibility is the adoption of corona resistant insulation systems, already used in high voltage machines. This solution may however require the use of thicker insulating layers, reducing fill factor and thus the power density. In addition, despite their good performance, it is probably not wise to design an insulation with PDIV lower than the peak voltage in service: the large switching frequencies of SiC-based inverters will probably destroy the insulation quickly.

Another possibility is the encapsulation of the end-winding or of the complete stator. Indusry has an experience in producing potting resins able to manage large swings in temperature (from $-55\,^{\circ}\mathrm{C}$ to $+155\,^{\circ}\mathrm{C}$ are common in the automotive sector). Therefore, it would not be a technological challenge but this solution will come at a cost. The actuator weight will be increased whereas the thermal conductivity will be decreased raising the temperature in the end-windings.

Finally, the machine design can be revised using form wound windings comprising conductors with rectangular cross section, i.e. hairpin technology. This permits to clearly define the specific location of the conductors within the slots, thus reducing the electrical stress between adjacent conductors. This solution has been already widely adopted for high voltage machines, whereas the application to low voltage motors is limited to certain sectors, where a high level of automation in the manufacturing process is required, such as in the automotive industry, and electrical machines are supplied with a low fundamental frequency.

In the aerospace sectors, the supply frequency of electrical machines is in general higher than in automotive, since, for a given target power, a higher electrical speed implies a reduced torque and reduced volume and weight for the machine. Conventional hairpin windings do not perform well at high frequency, as proximity and skin effects contribute to increase the equivalent winding resistance (AC resistance) and thus power losses, preventing their use in such applications.

However, innovative hairpin solutions, which minimize power losses at high frequency, have been proposed in [33] and [34], with promising results also for the aerospace sector.

VII. CONCLUSION

Partial discharge phenomena in insulation systems for machines used in the context of the More Electrical Aircraft were discussed in this series of papers. The aim was threefold: (a) to determine the electrical stress in the insulation through an accurate propagation model, (b) to highlight the behavior of insulation system subjected to wide bandgap impulse voltages and reduced pressures, (c) present some practical guidelines to ensure the insulation reliability.

The propagation model presented the Part I [3] can predict the electrical stress levels acting on a stator in an accurate fashion, accounting for both the overvoltage at the machine terminals and the voltage distribution within windings. The results provided for the reference system considered in [3] show that assuming a reflection coefficient equal to two (worst case) can largely overestimate the voltage at the machine terminals, leading to a too conservative design of the insulation.

In the Part II [4], the effect of fast transients on the PDIV has been studied, using a SiC inverter, varying frequency and rise time of the pulses. The results prove that SiC inverter impulse voltages do not modify the PDIV, facilitating stator testing as conventional impulse voltage generator can be used. To deal with the typical conditions of aircraft actuators, the dependence of PDIV on pressure and temperature is accounted by a single model provided that the permittivity of the dielectric is not affected significantly by temperature.

In this last Part III, it has been shown that to achieve a reliable system operation the insulation materials must be selected prioritizing the PDIV maximization and aiming the

enhancement of resin performance, also at elevated temperature. Additionally, it has been highlighted that, due to the elongation of the discharge field lines, using thicker insulation can have a moderate impact in improving the PDIV at reduced pressures. The same phenomenon helps reducing the impact of the aging, typically associated with thickness reduction. These results can be used to derive guidelines for testing complete stators and avoid partial discharge inception. These guidelines adapt the IEC 60034-18-41 to the context of aircraft application.

Combining the results from the first two parts provides figures that can be challenging using conventional two or three-level converters with 540 V dc bus voltage (±270 V architecture), especially for the turn-turn voltage like in the working case explored here. Looking forward, if voltages higher than ±270 V were used, solutions to enhance the PDIV would be needed. Possible alternatives have been discussed. At the actual state, it is not possible to identify an optimal solution among these, whereas a combination of them would probably lead to the best performance in term of reliability and efficiency of the drive system. New hairpin structures for the windings, used in conjunction with non-standard converter architectures, will probably be the way forward to enable the full potential of SiC devices to be exploited in aerospace systems.

REFERENCES

[1] M. Kaufhold, H. Aninger, M. Berth, J. Speck, and M. Eberhardt, "Electrical stress and failure mechanism of the winding insulation in PWM-inverter-fed low-voltage induction motors," *IEEE Trans. Ind. Electron.*, vol. 47, no. 2, pp. 396–402, Apr. 2000, doi: 10.1109/41.836355.

[2] W. Yin, "Failure mechanism of winding insulations in inverter-fed motors," *IEEE Elect. Insul. Mag.*, vol. 13, no. 6, pp. 18–23, Nov. 1997, doi: 10.1109/57.637150.

[3] M. Pastura, S. Nuzzo, F. Immovilli, A. Toscani, A. Rumi, A. Cavallini, G. Franceschini, and D. Barater, "Partial discharges in electrical machines for the more electric aircraft. Part I: A comprehensive modelling tool for the characterization of electric drives based on fast switching semiconductors," *IEEE Access*, to be published, doi: 10.1109/ACCESS.2021.3058083.

[4] L. Lusuardi, A. Rumi, A. Cavallini, D. Barater, and S. Nuzzo, "Partial discharge phenomena in electrical machines for the more electrical aircraft. Part II: Impact of reduced pressures and wide bandgap devices," *IEEE Access*, to be published, doi: 10.1109/ACCESS.2021.3058089.

[5] A. Hilal, B. Cougo, and T. Meynard, "Characterization of high power SiC modules for more electrical aircrafts," in *Proc. 42nd Annu. Conf. IEEE Ind. Electron. Soc. (IECON)*, Oct. 2016, pp. 1087–1092, doi: 10.1109/IECON.2016.7794111.

[6] R. A. Mastromauro, M. C. Poliseno, S. Pugliese, F. Cupertino, and S. Stasi, "SiC MOSFET dual active bridge converter for harsh environment applications in a more-electric-aircraft," in *Proc. Int. Conf. Electr. Syst. Aircr., Railway, Ship Propuls. Road Vehicles (ESARS)*, Mar. 2015, pp. 1–6, doi: 10.1109/ESARS.2015.7101427.

[7] A. Nawawi, R. Simanjorang, C. J. Gajanayake, A. K. Gupta, C. F. Tong, S. Yin, A. Sakanova, Y. Liu, Y. Liu, M. Kai, K. Y. See, and K.-J. Tseng, "Design and demonstration of high power density inverter for aircraft applications," *IEEE Trans. Ind. Appl.*, vol. 53, no. 2, pp. 1168–1176, Mar. 2017, doi: 10.1109/TIA.2016.2623282.

[8] S. Yin, K. J. Tseng, R. Simanjorang, Y. Liu, and J. Pou, "A 50-kW high-frequency and high-efficiency SiC voltage source inverter for more electric aircraft," *IEEE Trans. Ind. Electron.*, vol. 64, no. 11, pp. 9124–9134, Nov. 2017, doi: 10.1109/TIE.2017.2696490.

[9] *Rotating Electrical Machines—Part 18-41: Partial Discharge Free Electrical Insulation Systems (Type I) Used in Rotating Electrical Machines Fed From Voltage Converters—Qualification and Quality Control Tests*, IEC Standard 60034-18-41, 2019.

[10] G. G. Karady, M. D. Sirkis, and L. Liu, "Investigation of corona initiation voltage at reduced pressures," *IEEE Trans. Aerosp. Electron. Syst.*, vol. 30, no. 1, pp. 144–150, Jan. 1994, doi: 10.1109/7.250415.

[11] D. R. Meyer, A. Cavallini, L. Lusuardi, D. Barater, G. Pietrini, and A. Soldati, "Influence of impulse voltage repetition frequency on RPDIV in partial vacuum," *IEEE Trans. Dielectr. Electr. Insul.*, vol. 25, no. 3, pp. 873–882, Jun. 2018, doi: 10.1109/TDEI.2018.006722.

[12] L. Lusuardi, A. Rumi, G. Neretti, P. Seri, and A. Cavallini, "Assessing the severity of partial discharges in aerospace applications," in *Proc. IEEE Conf. Electr. Insul. Dielectr. Phenomena (CEIDP)*, Oct. 2019, pp. 267–270, doi: 10.1109/CEIDP47102.2019.9009970.

[13] A. Cavallini, "Reliability of low voltage inverter-fed motors: What have we learned, perspectives, open points," in *Proc. Int. Symp. Electr. Insulating Mater. (ISEIM)*, vol. 1, Sep. 2017, pp. 13–22, doi: 10.23919/ISEIM.2017.8088680.

[14] L. Lusuardi, A. Cavallini, M. G. de la Calle, J. M. Martinez-Tarifa, and G. Robles, "Insulation design of low voltage electrical motors fed by PWM inverters," *IEEE Elect. Insul. Mag.*, vol. 35, no. 3, pp. 7–15, May 2019, doi: 10.1109/MEI.2019.8689431.

[15] *Rotating Electrical Machines—Part 27-1: Off-Line Partial Discharge Measurements on the Winding Insulation*, Standard IEC 60034-27-1, 2017.

[16] *Rotating Electrical Machines—Part 27-5: Off-Line Partial Discharge Tests on Winding Insulation of Rotating Electrical Machines During Repetitive Impulse Voltage Excitation*, Standard IEC TS 60034-27-5 ED1, 2020.

[17] *Evaluation and Qualification of Electrical Insulation Systems*, Standard IEC 60505, 2011.

[18] *Rotating Electrical Machines—Part 18-21: Functional Evaluation of Insulation Systems—Test Procedures for Wire-Wound Windings—Thermal Evaluation and Classification*, Standard IEC 60034-18-21, 2012.

[19] P. Mancinelli, S. Stagnitta, and A. Cavallini, "Qualification of hairpin motors insulation for automotive applications," *IEEE Trans. Ind. Appl.*, vol. 53, no. 3, pp. 3110–3118, May 2017, doi: 10.1109/TIA.2016.2619670.

[20] L. Lusuardi, A. Cavallini, A. Caprara, F. Bardelli, and A. Cattazzo, "The impact of test voltage waveform in determining the repetitive partial discharge inception voltage of type I turn/turn insulation used in inverter-fed induction motors," in *Proc. IEEE Electr. Insul. Conf. (EIC)*, Jun. 2018, pp. 478–481, doi: 10.1109/EIC.2018.8481018.

[21] D. Fabiani, A. Cavallini, and G. C. Montanari, "A UHF technique for advanced PD measurements on inverter-fed motors," *IEEE Trans. Power Electron.*, vol. 23, no. 5, pp. 2546–2556, Sep. 2008, doi: 10.1109/TPEL.2008.2002069.

[22] *Winding Wires—Test Methods—Part 5: Electrical Properties*, IEC Standard 60851-5, 2008.

[23] *High-Voltage Test Techniques—Partial Discharge Measurements*, IEC Standard 60270, 2015.

[24] L. H. Ford, "The effect of humidity on the calibration of precision air capacitors," *J. Inst. Electr. Eng. II, Power Eng.*, vol. 95, no. 48, pp. 709–712, Dec. 1948, doi: 10.1049/ji-2.1948.0199.

[25] *IAGOS: In-Service Aircraft for a Global Observing System*. Accessed: Jul. 8, 2020. [Online]. Available: https://www.iagos.org/

[26] M. Pastura, S. Nuzzo, M. Kohler, and D. Barater, "Dv/Dt filtering techniques for electric drives: Review and challenges," in *Proc. 45th Annu. Conf. IEEE Ind. Electron. Soc. (IECON)*, Lisbon, Portugal, Oct. 2019, pp. 7088–7093, doi: 10.1109/IECON.2019.8926663.

[27] Y. Jiang, C. Feng, Z. Yang, X. Zhao, and H. Li, "A new active gate driver for MOSFET to suppress turn-off spike and oscillation," *Chin. J. Electr. Eng.*, vol. 4, no. 2, pp. 43–49, Jun. 2018, doi: 10.23919/CJEE.2018.8409349.

[28] P. Nayak and K. Hatua, "Active gate driving technique for a 1200 V SiC MOSFET to minimize detrimental effects of parasitic inductance in the converter layout," *IEEE Trans. Ind. Appl.*, vol. 54, no. 2, pp. 1622–1633, Mar. 2018, doi: 10.1109/TIA.2017.2780175.

[29] S. Lee and K. Nam, "An overvoltage suppression scheme for AC motor drives using a half DC-link voltage level at each PWM transition," *IEEE Trans. Ind. Electron.*, vol. 49, no. 3, pp. 549–557, Jun. 2002, doi: 10.1109/TIE.2002.1005379.

[30] T. Fuchslueger, H. Ertl, and M. A. Vogelsberger, "Reducing dv/dt of motor inverters by staggered-edge switching of multiple parallel sic half-bridge cells," in *Proc. PCIM Eur. Int. Exhib. Conf. Power Electron., Intell. Motion, Renew. Energy Energy Manage.*, 2017, pp. 1–8.

[31] D. Barater, J. Arellano-Padilla, and C. Gerada, "Incipient fault diagnosis in ultrareliable electrical machines," *IEEE Trans. Ind. Appl.*, vol. 53, no. 3, pp. 2906–2914, May 2017, doi: 10.1109/TIA.2017.2660465.

[32] D. Barater, G. Buticchi, C. Gerada, and J. Arellano-Padilla, "Diagnosis of incipient faults in PMSMs with coaxially insulated windings," in *Proc. 39th Annu. Conf. IEEE Ind. Electron. Soc. (IECON)*, Vienna, Austria, Nov. 2013, pp. 2756–2761.
[33] A. Arzillo, P. Braglia, S. Nuzzo, D. Barater, G. Franceschini, D. Gerada, and C. Gerada, "Challenges and future opportunities of hairpin technologies," in *Proc. IEEE 29th Int. Symp. Ind. Electron. (ISIE)*, Delft, The Netherlands, Jun. 2020, pp. 277–282.
[34] M. S. Islam, I. Husain, A. Ahmed, and A. Sathyan, "Asymmetric bar winding for high-speed traction electric machines," *IEEE Trans. Transport. Electrific.*, vol. 6, no. 1, pp. 3–15, Mar. 2020.

ALBERTO RUMI (Student Member, IEEE) was born in Lugo, Italy, in April 1994. He received the B.Sc. and M.S. degrees in electrical engineering from the University of Bologna, Italy, in July 2016 and March 2019, respectively, where he is currently pursuing the Ph.D. degree in biomedical, electrical and systems engineering. His research interests include diagnosis of insulation systems by partial discharge analysis, the study of the ageing mechanisms of rotating electrical machines, and reliability of inverter-fed low voltage motors, especially in the aeronautical and automotive fields.

LUCA LUSUARDI (Member, IEEE) was born in September 1991. He received the B.Sc. degree in energy engineering, the M.Sc. degree in energy and nuclear engineering, and the Ph.D. degree in biomedical, electrical and systems engineering from the University of Bologna, in 2013, 2016, and 2019, respectively. In June 2017, he joined IEEE Dielectrics and Electrical Insulation Society. In 2019, he was a Visiting Researcher with the University of Nottingham, U.K. Since December 2019, he has been working with the Research and Development Team, Rhiva AG (born from a detachment of the E-mobility group of Thyssenkrupp Presta AG), as the responsible of electrical insulation of electric powertrains. His research interests include design, analysis, and thermal management of electrical machines and drives, diagnosis of insulation systems by partial discharge analysis, and reliability modeling of inverter-fed low voltage motors.

ANDREA CAVALLINI (Senior Member, IEEE) was born in December 1963. He received the master's and Ph.D. degrees in electrical engineering from the University of Bologna, in 1990 and 1995, respectively. From 1995 to 1998, he was a Researcher with the University of Ferrara. Since 1998, he has been an Associate Professor with the University of Bologna. He was Co-Founder of Spinoff Company Techimp HQ Spa. He is the author or the coauthor of more than 250 international articles and holds 16 international patents. His research interests include diagnosis of insulation systems by partial discharge analysis and reliability of electrical systems and artificial intelligence. He is a member of IEC TC 2/MT 10.

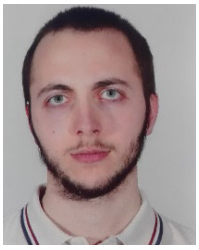

MARCO PASTURA received the M.Sc. degree in electrical engineering from The University of Pavia, Pavia, Italy, in 2018. He is currently pursuing the Ph.D. degree in automotive engineering for intelligent mobility with the Department of Engineering "Enzo Ferrari," University of Modena and Reggio Emilia, Modena, Italy. His research interest includes the electrical drives for automotive and aerospace applications with focus on high reliability electrical machines.

DAVIDE BARATER (Member, IEEE) received the master's degree in electronic engineering and the Ph.D. degree in information technology from the University of Parma, Italy, in 2009 and 2014, respectively.

In 2012, he was an Honorary Scholar with the University of Nottingham, U.K., and a Visiting Researcher with the University of Kiel, in 2015. He is currently an Assistant Professor with the Department of Engineering "Enzo Ferrari," University of Modena and Reggio Emilia, Italy. He is the Coordinator of two European projects: 1) RAISE, that evaluates the impact of the high voltage gradients, introduced by the fast commutations of new wide bandgap power devices (SiC, GaN), on the life time of electrical motor insulation systems; and 2) AUTO-MEA, that aims to develop electrical motors and drives for next generation of electrical mobility. In particular, novel solutions for windings structures and cooling systems for improved power density, efficiency and increased frequency operation. He is the author or the coauthor of more than 60 international articles. His research interest includes power electronics for e-mobility and motor drives.

Dr. Barater is an Associate Editor of IEEE TRANSACTIONS ON INDUSTRY APPLICATIONS.

STEFANO NUZZO (Member, IEEE) received the B.Sc. and M.Sc. degrees in electrical engineering from the University of Pisa, Pisa, Italy, in 2011 and 2014, respectively, and the Ph.D. degree in electrical engineering from the University of Nottingham, Nottingham, U.K, in 2018. He worked as a Research Fellow with the Power Electronics, Machines and Control (PEMC) Group, University of Nottingham. Since January 2019, he has been a Research Fellow with the Department of Engineering "Enzo Ferrari," University of Modena and Reggio, Modena, Italy. He is also involved in a number of projects related to the more electric aircraft initiative and associated fields. His research interest includes the analysis, modeling and optimizations of electrical machines, with focus on salient-pole synchronous generators and brushless excitation systems for industrial power generation applications.

He is a Member of the IEEE Industrial Electronics Society (IES) and the IEEE Industry Applications Society (IAS). He constantly serves the scientific community as a reviewer for several journals and conferences.